The Canadian Mineralogist
Vol. 40, pp. 1451-1463 (2002)

PALLADIUM AND PLATINUM MINERALS FROM THE SERRA PELADA Au–Pd–Pt DEPOSIT, CARAJÁS MINERAL PROVINCE, NORTHERN BRAZIL

ALEXANDRE RAPHAEL CABRAL[§] AND BERND LEHMANN

Institut für Mineralogie und Mineralische Rohstoffe, Technische Universität Clausthal, Adolph-Roemer-Str. 2A, D–38678 Clausthal-Zellerfeld, Germany

ROGERIO KWITKO-RIBEIRO

Centro de Desenvolvimento Mineral, Companhia Vale do Rio Doce, BR 262/ km 296, 33030-970 Santa Luzia – MG, Brazil

CARLOS HENRIQUE CRAVO COSTA

Diretoria de Metais Nobres, Companhia Vale do Rio Doce, Caixa Postal 51, Serra dos Carajás, 68516-000 Parauabepas – PA, Brazil

ABSTRACT

The Serra Pelada *garimpo* (1980–1984) was the site of the most spectacular gold rush in recent history, but the mineralogy of the bonanza-style mineralization has not so far been documented in detail. Rediscovery of an early drill-core, recovered in 1982 from the near-surface lateritic portion of the *garimpo* area, has provided coarse-grained gold aggregates for this study. The centimeter-long aggregates of gold occur in powdery, earthy material. They exhibit a delicate arborescent fabric and are coated by goethite. Four compositional types of gold are recognized: palladian gold with an atomic ratio Au:Pd of 7:1 ("Au_7Pd"), Hg-bearing palladian gold (Au–Pd–Hg), Pd-bearing gold with up to 3 wt.% Pd (Pd-poor gold) and pure gold. A number of platinum-group minerals (*PGM*) are included in, or attached to the surface of, palladian gold: "guanglinite", Sb-bearing "guanglinite", atheneite and isomertieite, including the noteworthy presence of Se-bearing *PGM* (Pd–Pt–Se, Pd–Se, Pd–Hg–Se and Pd–Bi–Se phases, and sudovikovite and palladseite). They define an As–Sb–Hg–Se mineral assemblage typical of hydrothermal vein-type deposits formed at relatively low temperatures. Native palladium, characteristically situated in the goethite coating, is intimately associated with a Pd–O phase. The remarkable occurrence of native platinum associated with Pd-bearing gold, *PGM* (compositionally close to mertieite-II and isomertieite) and berzelianite from a nearby prospect (Elefante prospect) is also recorded.

Keywords: palladian gold, platinum-group minerals, Pd–O phase, native palladium, native platinum, Serra Pelada *garimpo*, Carajás mineral province, Brazil.

SOMMAIRE

Le *garimpo* de Serra Pelada (1980–1984) a été le site de la ruée vers l'or la plus spectaculaire en temps modernes, mais la minéralogie de cette minéralisation de style bonanza n'a pas encore fait l'objet d'une étude détaillée. La redécouverte d'une carotte forée en 1982 d'un profil latéritique du *garimpo* nous a permis d'échantillonner des aggrégats d'or à grains grossiers. Ces aggrégats, d'une taille centimétrique, se présentent dans un matériau pulvérulent. Ils possèdent une forme arborescente délicate et sont recouverts d'une gaine de goethite. Nous distinguons quatre types d'or selon leur composition: or palladifère ayant un rapport atomique Au:Pd de 7:1 ("Au_7Pd"), or palladifère et mercurifère (Au–Pd–Hg), or palladifère contenant jusqu'à 3% de Pd en poids (or à faible teneur en Pd) et or pur. Plusieurs minéraux du groupe du platine sont inclus dans l'or palladifère, ou bien rattachés à la surface de ces grains: "guanglinite", "guanglinite" stibifère, athénéite et isomertiëite, avec la présence notoire de phases sélénifères (Pd–Pt–Se, Pd–Se, Pd–Hg–Se et Pd–Bi–Se, ainsi que sudovikovite et palladséite). Ces minéraux définissent un assemblage As–Sb–Hg–Se typique de gisements hydrothermaux en veines, formés à températures relativement faibles. Le

§ *E-mail address*: cabral@min.tu-clausthal.de

palladium natif, caractéristiquement inclus dans la gaine de goethite, est intimement lié à une phase Pd–O. Nous soulignons aussi l'association remarquable de platine natif associé à l'or palladifère, des minéraux du groupe du platine dont la composition se rapproche de celle de la mertiëite-II et de l'isomertiëite, et berzélianite provenant de Elefante, puit d'exploration voisin.

(Traduit par la Rédaction)

Mots-clés: or palladifère, minéraux du groupe du platine, phase Pd–O, palladium natif, platine natif, *garimpo* Serra Pelada, province minérale de Carajás, Brésil.

Introduction

Discovered in 1980 by *garimpeiros*, the Serra Pelada gold deposit was soon reputed to be an eldorado in the Amazon region. Its gold, characteristically coarse-grained and alloyed with palladium (Meireles & Silva 1988), was completely mined out from the near-surface lateritic portion, where it occurred as bonanza ore in disaggregated, quartz-bearing clayey material. The *garimpo* (open pit) collapsed and flooded in 1984. According to Meireles & Silva (1988), 32.6 tonnes of gold were extracted, but unofficial figures place the amount closer to 70 tonnes of gold.

A drill core recovered in 1982 from the central part of the Serra Pelada *garimpo* is the only relic of the near-surface bonanza ore. One depth interval of this drill core (SP–32, 54.5–55.0 m at 132,000 g/t Au, 11,400 g/t Pd, 359 g/t Pt) (Cabral *et al.* 2002a) has provided coarse-grained aggregates of dendritic gold for investigation. Because the coarse-grained gold was recovered from disaggregated and powdery material, supergene enrichment has been suggested to account for the bonanza grade (Tallarico *et al.* 2000, Moroni *et al.* 2001). Our contribution records what seems to be a hydrothermal assemblage of palladium minerals associated with coarse-grained palladian gold. A native platinum vein-type mineralization from a nearby prospect, known as "Elefante", also is documented.

Geological Setting and the Serra Pelada Deposit

Serra Pelada is one of the numerous ore deposits of the Carajás mineral province (Fig. 1). Reviews of the geological setting of the Carajás mineral province can be found elsewhere (*e.g.,* Docegeo 1988, Villas & Santos 2001, Moroni *et al.* 2001), and only a brief account of the Serra Pelada Au–Pd–Pt deposit is given here.

The deposit is hosted by the Rio Fresco Formation, a fluvial to shallow marine sequence of Late Archean age, which comprises weakly metamorphosed conglomerate, sandstone, dolomitic marble and siltstone. That formation is underlain by the volcano-sedimentary Rio Novo Sequence (Cunha *et al.* 1984, Meireles & Silva 1988, Docegeo 1988, Tallarico *et al.* 2000), whose age is constrained by the intrusive, chromite- and PGE-mineralized Luanga layered mafic–ultramafic complex (2763 ± 6 Ma: Machado *et al.* 1991, Suita & Nilson 1988, Diella *et al.* 1995), a few kilometers east–southeast of Serra Pelada. All these rocks were affected by the reactivation (*ca*. 1.9 Ga) of the east–west-trending Cinzento strike-slip system (Pinheiro & Holdsworth 1997a), which is still active today with small-scale earthquakes and hot springs about 50 km west–northwest from Serra Pelada (Pinheiro & Holdsworth 1997b). Proterozoic magmatism is represented by the anorogenic Cigano Granite (1883 ± 2 Ma, Machado *et al.* 1991), exposed about 15 km west of Serra Pelada. Subordinate dioritic and granodioritic rocks of unknown age also occur in the area (Tallarico *et al.* 2000). The minimum age for the onset of weathering in the Carajás region, based on K–Ar and $^{40}Ar/^{39}Ar$ dating of K-bearing manganese oxides, is *ca.* 72 ± 6 Ma (Vasconcelos *et al.* 1994).

The near-surface bonanza ore occurs as brecciated, but completely disaggregated, quartz-bearing clayey masses. At depth, the mineralization is less friable and lacks the aggregates of coarse-grained, characteristically dendritic, palladian gold. Located in the deeply weathered hinge-zone of a recumbent syncline, the deep-seated mineralization consists of brecciated, fine-grained carbonaceous rocks with variable amounts of quartz, carbonaceous matter, white mica, kaolinite, hematite, goethite and manganese oxide (Tallarico *et al.* 2000, Moroni *et al.* 2001). It is surrounded by a 5- to 50-m-thick zone of silicification, and broadly follows the contact between dolomitic marble and carbonaceous metasiltstone of the Rio Fresco Formation (Tallarico *et al.* 2000).

Analytical Techniques

Coarse-grained aggregates of gold (1–3 cm across) were picked from the drill core SP–32 at the depth interval of 54.5–55.0 m. After removal of the powdery clayey material, the gold aggregates were investigated by scanning electron microscopy (SEM). Polished sections were then prepared for ore microscopy and electron-microprobe analysis with a Cameca SX100 at the TU Clausthal. Analytical conditions, X-ray emission lines and standards were the same as described in Cabral *et al*. (2001), with the exception of platinum and selenium, now sought using the $L\alpha$ lines and pure metals as standards. Occasional modifications in the X-ray emission lines and analytical conditions used are noted in the tables.

Palladium and Platinum Minerals from Serra Pelada

Platinum-group minerals (*PGM*) are associated with coarse-grained gold, which occurs as cm-long dendrites roughly 1 mm thick (Fig. 2a) and as wire-haired aggregates of arborescent fabric (Fig. 2b). The crystals of gold are usually coated with goethite (Fig. 3a). At the contact between gold crystals and the goethite coating, it is common to observe masses of native palladium intermingled with a Pd–O phase (Fig. 3b). The coarse-grained crystals of gold occasionally host subhedral to euhedral inclusions (5–20 μm in length) of palladium- and platinum-bearing minerals (Fig. 3c). Where closely associated with goethite, the *PGM* commonly have a low-reflectance alteration-induced halo consisting of a Pd–O phase (Fig. 3d).

Reconnaissance electron-microprobe work has indicated a uniform content of about 7 wt.% Pd in gold crystals. They have an empirical stoichiometry of Au_7Pd (Table 1) (Cabral *et al.* 2002a). However, the composition of gold is not ubiquitously uniform. Systematic investigation has shown that the gold composition is variable in terms of both palladium, from 1.6 to 9.8 wt.% Pd, and mercury, up to 1.5 wt.% Hg (Table 1). Consequently, three compositional types of palladian gold are distinguished in this study (Serra Pelada only): (i) gold alloy with about 7 wt.% Pd, (ii) Hg-bearing Au–Pd alloys with >3 wt.% Pd, and (iii) Au–Pd alloys with <3 wt.% Pd. They will be referred to as "Au_7Pd", Au–Pd–Hg and Pd-poor gold, respectively. The term "palladian gold" is used here to designate any Au–Pd alloy. All these Au–Pd alloys are virtually free of silver. Under reflected light, the Au–Pd crystals show a whitish yellow color.

Palladium-free gold also is present, but in insignificant amounts compared to the palladian gold. It is readily distinguished from Au–Pd alloys by its typical yellow color. Being virtually pure (Table 2), the yellow gold occurs as veinlets and tiny crystals (<5 μm across) near the margin of, and attached to, crystals of palladian gold.

Specific assemblages of *PGM* are associated with the compositional types of palladian gold (Table 3). By far, "Au_7Pd" is the dominant compositional type in the 13 aggregates of gold studied. Where present, the most abundant mineral inclusions in the coarse-grained dendrites of "Au_7Pd" are two palladium arsenides (Table 4). One is Sb-free and contains around 19 wt.% As (Fig. 3c). The Pd:As ratio indicates stoichiometric Pd_3As, corresponding to "guanglinite", not an IMA-approved name (Cabri & Laflamme 1981, p. 159). The other arsenide has some antimony in the range of 4.3–4.6 wt.% Sb at the expense of arsenic, and hence maintains the same stoichiometry, that is $Pd_3(As,Sb)$, an Sb-bearing "guanglinite". Other inclusions are a (i) Pd–Pt–Se and

TABLE 1. ELECTRON-MICROPROBE DATA ON PALLADIAN GOLD,* SERRA PELADA Au–Pd–Pt DEPOSIT, NORTHERN BRAZIL

	Au	Pd	Hg	Ag	Cu	Fe	Total	Au	Pd	Hg	Ag	Cu	Fe
				wt.%				On the basis of 8 atoms					
1	92.31	7.52	<0.2	<0.3	<0.07	<0.05	99.83	6.952	1.048	----	----	----	----
2	92.77	7.30	<0.2	<0.3	<0.07	<0.05	100.07	6.983	1.017	----	----	----	----
3	92.65	7.33	<0.2	<0.3	<0.07	<0.05	99.98	6.978	1.022	----	----	----	----
4	92.57	7.37	<0.2	<0.3	<0.07	<0.05	99.94	6.973	1.027	----	----	----	----
5	92.93	6.92	<0.2	<0.3	<0.07	<0.05	99.85	7.031	0.969	----	----	----	----
6	92.56	7.28	<0.2	<0.3	<0.07	<0.05	99.84	6.983	1.017	----	----	----	----
7	92.37	7.78	<0.2	<0.3	<0.07	<0.05	100.15	6.921	1.079	----	----	----	----
8	92.52	7.32	<0.2	<0.3	<0.07	<0.05	99.84	6.978	1.022	----	----	----	----
9	92.73	7.39	<0.2	<0.3	<0.07	<0.05	100.12	6.972	1.028	----	----	----	----
10	93.09	7.25	<0.2	<0.3	<0.07	<0.05	100.34	6.992	1.008	----	----	----	----
11	92.51	7.60	<0.2	<0.3	<0.07	<0.05	100.11	6.944	1.056	----	----	----	----
12	92.59	7.51	<0.2	<0.3	<0.07	<0.05	100.10	6.956	1.044	----	----	----	----
13	93.09	7.05	<0.2	<0.2	0.13	<0.05	100.27	6.990	0.980	----	----	0.030	----
14	93.10	6.98	<0.2	<0.2	0.08	<0.05	100.16	7.009	0.973	----	----	0.019	----
15	92.76	7.31	<0.2	0.22	<0.07	<0.05	100.29	6.955	1.014	----	0.030	----	----
								On the basis of 1 atom					
16	91.74	5.72	1.54	<0.3	0.58	<0.05	99.58	0.868	0.100	0.014	----	0.017	----
17	87.42	9.76	1.47	<0.3	0.58	<0.05	99.23	0.804	0.166	0.013	----	0.017	----
18	92.06	5.81	0.64	<0.3	0.68	<0.05	99.19	0.872	0.102	0.006	----	0.020	----
19	95.06	3.21	0.31	<0.3	0.67	<0.05	99.25	0.919	0.057	0.003	----	0.020	----
20	94.29	4.34	0.62	<0.3	0.62	<0.05	99.87	0.899	0.077	0.006	----	0.018	----
21	96.24	2.44	<0.2	0.34	0.60	<0.05	99.62	0.932	0.044	----	0.006	0.018	----
22	96.59	2.00	<0.2	0.36	0.59	0.12	99.66	0.936	0.036	----	0.006	0.018	0.004
23	98.06	1.61	<0.2	0.38	0.56	<0.05	100.61	0.948	0.029	----	0.007	0.017	----
24	96.94	1.99	<0.2	0.36	0.54	<0.05	99.83	0.942	0.036	----	0.006	0.016	----
25	96.86	1.92	<0.2	0.34	0.61	0.09	99.82	0.938	0.034	----	0.006	0.018	0.003

* Drill core SP–32, 54.5–55.0 m. The results correspond to the following compositional types of gold, referred to in the text: 1–15: "Au_7Pd", 16–20: Au–Pd–Hg, 21–25: Pd-poor gold. The compositions are first listed in terms of wt%, then expressed in terms of atoms per formula unit, *apfu*.

(ii) Pd–Se phases and, more rarely, selenides analogous to (iii) sudovikovite, $PtSe_2$ (Fig. 3c), and (iv) palladseite, $Pd_{17}Se_{15}$. The Pd–Pt–Se phase has about 72–75 wt.% Pd and a Pt:Se ratio of approximately 1:2, indicating an empirical stoichiometry of Pd_9PtSe_2 (Cabral *et al.* 2002a). Palladseite and sudovikovite are found as tiny (<5 μm in diameter), subhedral crystals; the former is Hg-bearing (Cabral *et al.* 2002a). The Pd–Se phase occurs as subhedral to anhedral crystals 5–20 μm in length and is usually surrounded by a Hg-bearing Pd–O phase (Fig. 3d). Being essentially composed of about 85 wt.% Pd and 14 wt.% Se, this phase has a Pd:Se ratio of about

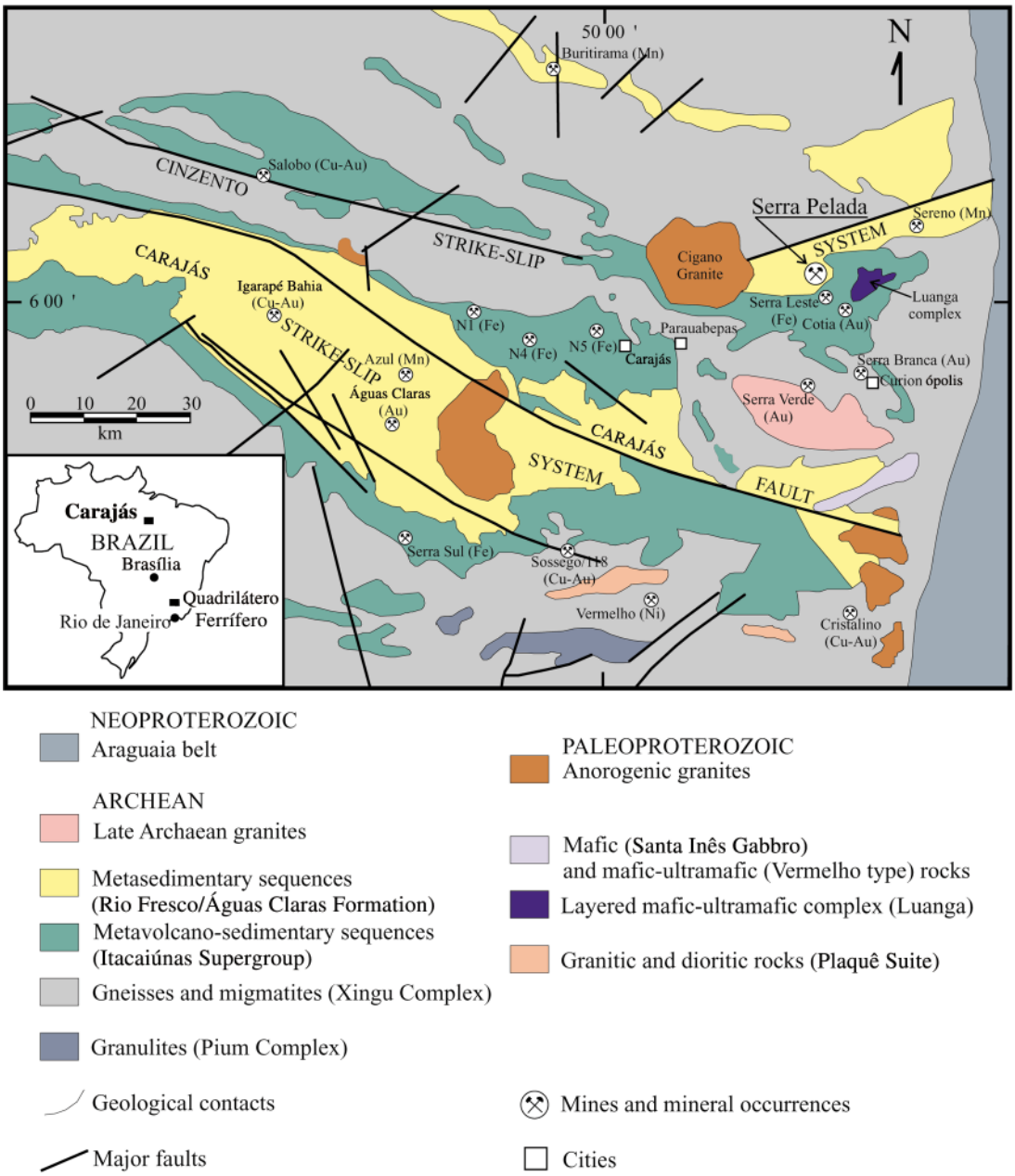

FIG. 1. Simplified geological map of the Carajás mineral province (Dardenne & Schobbenhaus 2001, and references therein).

4.5, close to the stoichiometry of the synthetic compound Pd_9Se_2 (Table 5).

Other *PGM* associated with the "Au_7Pd" dendrites are situated in the goethite coating. Of very restricted occurrence, these minerals are too small to avoid interference from either the goethite coating or the palladian gold. Therefore, their microprobe-derived compositions must be considered with caution (Table 6). They are: (i) a Pd–Pt–S–As–Se phase (Fig. 3a), (ii) a Pd–Au–Pt–As phase (Fig. 3b), and (iii) a Se-bearing Pt–Pd sulfide.

The Au–Pd–Hg alloy has a mineral assemblage characterized by a Pd–Hg–As phase. The Pd–Hg–As crystals are subhedral, 10–50 μm in length, commonly attached to the margins of the Hg-bearing palladian gold (Fig. 3e). Recalculation of the electron-microprobe data indicates an empirical stoichiometry close to that of atheneite, $(Pd,Hg)_3As$; some platinum, up to 2 wt.% Pt, has also been detected (Table 7). Other *PGM* apparently restricted to the Au–Pd–Hg alloy occur very rarely as subhedral crystals of about 10 μm in length: (i) a Pb-bearing Pd–Hg–Se phase, and (ii) a Pd–Bi–Se phase (Table 7).

The Pd-poor gold crystals are usually finer (<100 μm) than those of "Au_7Pd" and the Au–Pd–Hg alloy, but coarse-grained (>100 μm) crystals also exist. The

TABLE 3. COMPOSITIONAL TYPES OF GOLD AND RELATED MINERAL ASSEMBLAGES, SERRA PELADA Au–Pd–Pt DEPOSIT, NORTHERN BRAZIL

Compositional types		Mineral inclusions	Matrix minerals
"Au_7Pd"	Early hydrothermal	"guanglinite" Sb-bearing "guanglinite" Pd–Pt–Se phase Pd–Se phase palladseite sudovikovite diaspore?	native Pd* Pd–O phases* goethite xenotime
Au–Pd–Hg	Early hydrothermal	Pd–Bi–Se phase	atheneite* Pd–Hg–Se phase* romanèchite
Pd-poor Au	Late hydrothermal	isomertieite	isomertieite* romanèchite
Pure Au	Supergene		goethite

* The mineral phases are commonly situated on the surface of gold crystals, embedded in a matrix of Fe or Mn oxide minerals

TABLE 2. ELECTRON-MICROPROBE DATA ON YELLOW GOLD ASSOCIATED WITH PALLADIAN GOLD ("Au_7Pd"),* SERRA PELADA Au–Pd–Pt DEPOSIT, NORTHERN BRAZIL

	1	2	3	4	5
Au wt.%	99.70	99.59	98.90	99.27	99.22
Ag	<0.20	<0.20	0.22	0.32	0.31
Cu	<0.07	<0.07	<0.07	<0.07	<0.07
Fe	0.28	<0.05	0.33	0.32	0.10
Pd	0.10	<0.04	<0.04	<0.04	<0.04
Total	100.08	99.59	99.45	99.91	99.63
Au at.%	98.84	100.00	98.43	98.25	99.02
Ag	-----	-----	0.39	0.58	0.59
Cu	-----	-----	-----	-----	-----
Fe	0.98	-----	1.18	1.17	0.39
Pd	0.18	-----	-----	-----	-----

* Drill core SP-32, 54.5–55.0 m.

TABLE 4. ELECTRON-MICROPROBE DATA ON PALLADIUM ARSENIDE INCLUSIONS IN PALLADIAN GOLD ("Au_7Pd")*, SERRA PELADA Au–Pd–Pt DEPOSIT, NORTHERN BRAZIL

	1	2	3	4	5	6	7	8	9	10
Au wt.%	1.94	1.98	2.56	2.59	1.39	1.32	1.86	2.46	1.24	1.29
Pd	80.27	79.09	79.60	79.77	80.02	80.83	78.32	78.30	78.10	78.98
As	19.14	19.06	19.19	19.24	19.41	19.15	15.93	15.84	15.95	16.12
Sb	<0.03	<0.03	<0.03	<0.03	<0.03	<0.03	4.27	4.63	4.44	4.27
Total	101.35	100.13	101.35	101.60	100.82	101.30	100.38	101.23	99.73	100.66
Au *apfu*	0.039	0.040	0.051	0.051	0.028	0.027	0.036	0.048	0.024	0.026
Pd	2.959	2.951	2.942	2.942	2.955	2.972	2.965	2.953	2.968	2.972
As	1.001	1.009	1.007	1.008	1.018	1.001	0.858	0.847	0.861	0.862
Sb	-----	-----	-----	-----	-----	-----	0.141	0.152	0.146	0.140
ΣAs	1.001	1.009	1.007	1.008	1.018	1.001	0.999	0.999	1.007	1.002

* Drill core SP-32, 54.5–55.0 m.

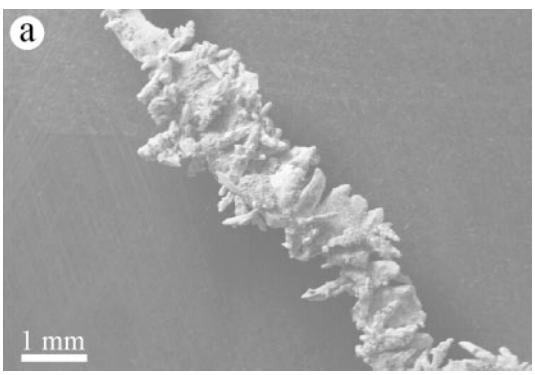

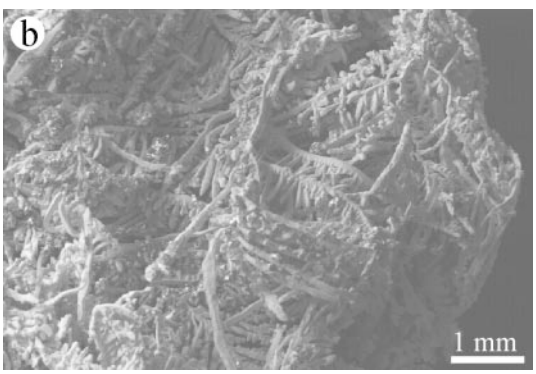

FIG. 2. SEM images of (a) a palladian gold thread and (b) an arborescent palladian gold aggregate from Serra Pelada.

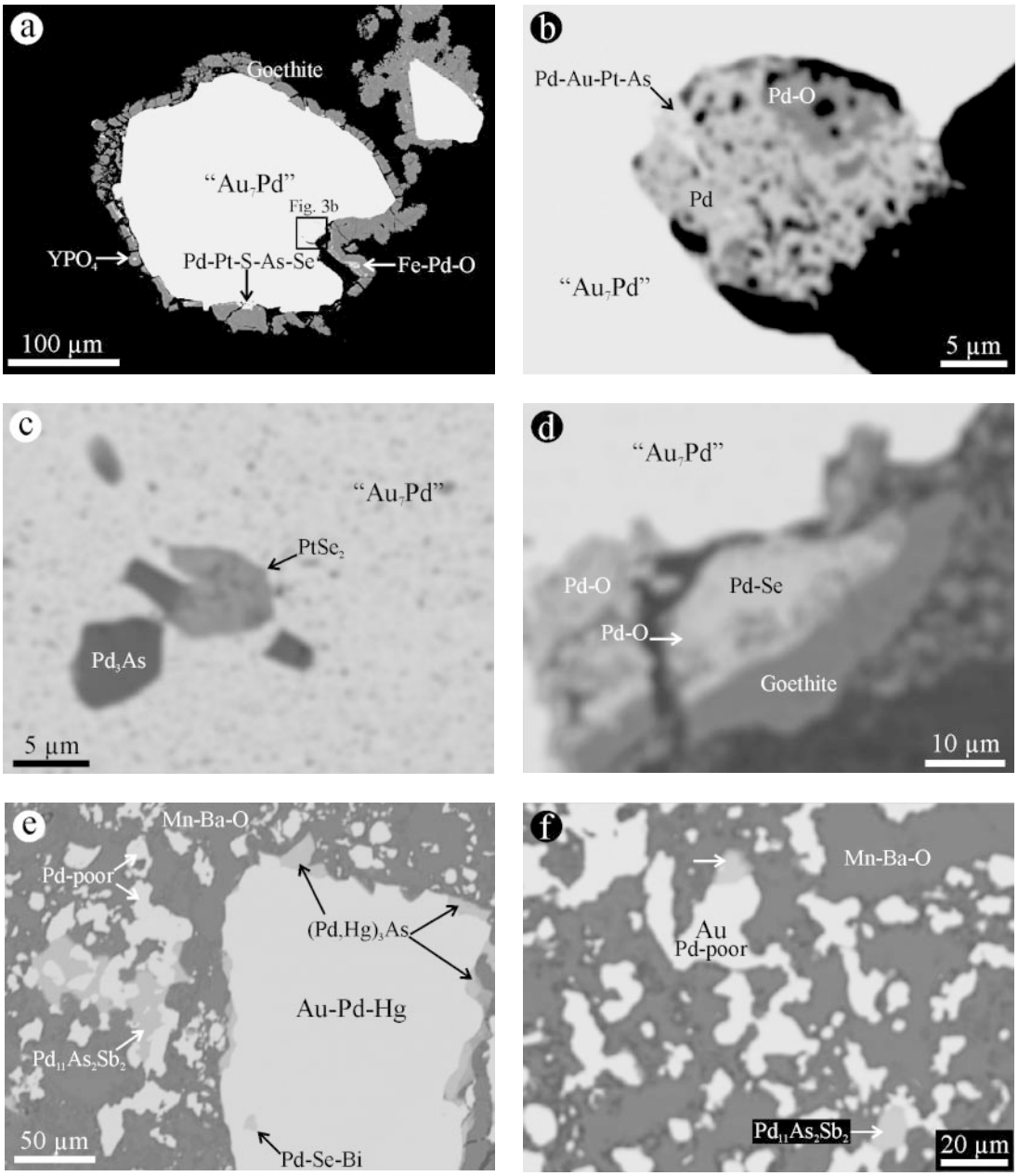

FIG. 3. Back-scattered electron (BSE) images of palladian gold and associated *PGM* from Serra Pelada. a. Crystals of palladian gold (empirical stoichiometry: "Au_7Pd") coated by goethite. Note inclusions of YPO_4 and Fe–Pd–O phase in the goethite coating. Electron-microprobe data for the Pd–Pt–S–As–Se phase are provided in Table 6 (anal. 1). Black: resin. b. Detail of the area indicated in (a). Native palladium (Pd) intimately associated with a Pd–O phase and a relic of a Pd?–Au?–Pt–As phase (Table 6, anal. 2). Black: resin. c. Inclusions of sudovikovite ($PtSe_2$) and "guanglinite" (Pd_3As) in palladian gold ("Au_7Pd"). d. Alteration rim of Pd–O on Pd–Se phase at the contact between palladian gold ("Au_7Pd") and goethite. Black: resin. e. Hg-bearing palladian gold (Au–Pd–Hg), Pd-poor gold and associated *PGM* in a Mn–Ba–O matrix (possibly romanèchite, dark grey). Note that the crystals of atheneite [$(Pd,Hg)_3As$] are on the surface of the Au–Pd–Hg alloy. f. Aggregates of Pd-poor gold and isomertieite ($Pd_{11}As_2Sb_2$, arrows) intergrown with a Mn–Ba oxide (romanèchite?, dark grey).

crystals of Pd-poor gold have so far been recognized in aggregates intergrown with a Mn–Ba oxide (Figs. 3f), possibly romanèchite, in which coarse-grained crystals of Au–Pd–Hg alloy occur (Fig. 3e). A Pd–As–Sb mineral seems to compose a particular mineral assemblage with the Pd-poor gold. The Pd–As–Sb crystals are subhedral and have a variable grain-size. Where fine-grained (<100 μm), they are found as aggregates with Pd-poor gold (Figs. 3e, f) and as isolated crystals; those slightly exceeding 100 μm in length are attached to coarse-grained Pd-poor gold. Their composition is about 75 wt.% Pd, 14% Sb and 9% As, corresponding to that of isomertieite, $Pd_{11}Sb_2As_2$ (Table 7).

Native palladium, Pd–O and gangue minerals

Native palladium is characteristically located at the contact between the goethite coating and "Au_7Pd". Two styles of occurrence are recognized: (i) as masses (Fig. 3b) and (ii) as submicrometer-wide stripes lining vugs (Fig. 4a). There is an intimate association between native palladium and a Pd–O phase of low reflectance, which imparts a spongy appearance to the palladium masses (Fig. 3b). Relics of *PGM* are sporadically found in masses of native palladium. The native palladium is generally pure (Table 8); the extraneous elements detected in micro-analyses may stem from the surroundings (Au from palladian gold) or be inherited from a precursor *PGM* (7.2 wt.% As, anal. 5, Table 8).

Apart from being intermingled with masses of native palladium, the low-reflectance, Pd–O phase also occurs as an alteration halo on *PGM*. Such halos are best developed on arsenic- and selenium-bearing palladium minerals where in contact with goethite (Fig. 3d). The Pd–Se phase of Figure 3d (no Hg and Cu detected) is altered to Pd–O with 2.0 wt.% Hg and 1.7 wt.% Cu. Some Pd–O-bearing phases were analyzed for oxygen. The oxidation-induced halo on the Pd–Pt–Se phase, for instance, has low contents of oxygen, from about 4 to 6 wt.% O; higher contents (9–11 wt.% O) were detected in the Pd–O associated with native palladium (Table 9). Note that in some cases, considerable amounts of Hg, Cu and Mn, and perhaps Cl, are present in the Pd–O phases.

Gangue minerals are rarely included in the "Au_7Pd" alloy. One exception is an acicular Al–O, possibly diaspore [AlO(OH)]. Rare crystals of yttrium phosphate (probably a xenotime-group mineral) occur in vugs

TABLE 5. ELECTRON-MICROPROBE DATA ON PALLADIUM–SELENIUM ALLOY,* SERRA PELADA Au–Pd–Pt DEPOSIT, NORTHERN BRAZIL

	1	2	3	4	5
Pd wt.%	85.01	84.89	84.96	85.05	84.64
Au	0.97	0.88	1.19	1.12	0.74
Fe	0.41	0.41	0.53	0.59	0.83
Se	13.61	14.18	13.99	14.24	14.17
S	0.03	<0.03	<0.03	<0.03	<0.03
Total	100.03	100.36	100.67	101.00	100.38
Pd *apfu*	8.926	8.871	8.861	8.828	8.807
Au	0.055	0.050	0.067	0.063	0.042
Fe	0.082	0.082	0.105	0.117	0.164
Σ*Pd*	9.063	9.003	9.033	9.008	9.013
Se	1.926	1.997	1.967	1.992	1.987
S	0.010	-----	-----	----	----

* Drill core SP–32, 54.5–55.0 m.

TABLE 6. ELECTRON-MICROPROBE DATA ON THE *PGM* AT THE CONTACT BETWEEN THE GOETHITE COATING AND PALLADIAN GOLD ("Au_7Pd"),* SERRA PELADA Au–Pd–Pt DEPOSIT, NORTHERN BRAZIL

	1	2	3		1	2	3
Au wt.%	<0.30	27.23	<0.30	Au *apfu*	-----	0.179	----
Pt	34.26	10.11	75.82	Pt	0.184	0.067	0.825
Cu	<0.07	0.09	<0.07	Cu	-----	0.002	----
Fe	1.01	0.09	0.80	Fe	0.019	0.002	0.030
Pd	50.74	58.77	5.51	Pd	0.500	0.716	0.110
As	7.58	1.80	<0.10	As	0.106	0.031	----
S	4.38	<0.03	15.36	S	0.143	-----	1.016
Se	3.64	0.18	0.69	Se	0.048	0.003	0.019
Total	101.61	98.27	98.18	Σ	1	1	2

* Drill core SP–32, 54.5–55.0 m.

TABLE 7. ELECTRON-MICROPROBE DATA ON PGM ASSOCIATED WITH Au–Pd–Hg and Pd-POOR GOLD ALLOYS,* SERRA PELADA Au–Pd–Pt DEPOSIT, NORTHERN BRAZIL

	1	2	3	4	5	6	7	8	9	10
Pd wt.%	67.15	68.18	67.90	67.04	68.76	63.06	75.25	74.89	75.63	75.46
Au	0.47	1.10	2.06	0.39	3.61	0.84	0.89	0.93	0.94	1.46
Hg	13.79	13.99	13.77	13.22	<0.2	11.70	<0.20	<0.20	<0.20	<0.20
Pt	1.96	<0.30	<0.30	1.62	0.35	<0.30	<0.30	<0.30	<0.30	<0.30
Cu	<0.07	<0.07	<0.07	<0.07	<0.07	<0.07	0.12	0.17	0.09	0.12
Fe	0.08	<0.05	0.07	0.22	<0.05	<0.05	0.12	<0.05	<0.05	<0.05
Pb	n.a.	n.a.	n.a.	n.a.	n.a.	4.43	n.a.	n.a.	n.a.	n.a.
As	17.48	16.94	16.90	18.30	<0.15	0.15	9.11	8.84	9.27	8.85
Sb	<0.03	<0.03	<0.03	<0.03	<0.03	<0.03	14.67	14.79	14.39	14.57
Sn	<0.03	<0.03	<0.03	<0.03	<0.03	<0.03	<0.03	<0.03	0.06	0.05
Se	<0.07	<0.07	<0.07	0.13	8.44	18.87	<0.07	<0.07	<0.07	<0.07
Bi	n.a.	n.a.	n.a.	n.a.	19.91	<0.50	n.a.	n.a.	n.a.	n.a.
Total	100.93	100.21	100.70	100.92	101.07	99.05	100.16	99.62	100.38	100.51
Pd *apfu*	2.665	2.720	2.704	2.636	2.976	2.583	11.075	11.105	11.113	11.119
Au	0.010	0.024	0.044	0.008	0.084	0.019	0.071	0.075	0.075	0.116
Hg	0.290	0.296	0.291	0.276	--	0.254	----	----	-----	-----
Pt	0.042	-----	-----	0.035	0.008	----	----	----	-----	-----
Cu	----	----	-----	-----	-----	-----	0.030	0.042	0.022	0.030
Fe	0.006	-----	0.005	0.016	-----	----	0.034	----	-----	-----
Pb	-----	----	----	----	----	0.093	-----	-----	-----	----
ΣPd	3.014	3.040	3.044	2.971	3.069	2.949	11.209	11.221	11.209	11.265
As	0.986	0.960	0.956	1.022	-----	0.009	1.904	1.862	1.935	1.852
Sb	-----	-----	-----	-----	-----	----	1.887	1.917	1.848	1.876
Sn	----	----	----	----	----	----	-----	-----	0.008	0.007
Se	-----	-----	-----	0.007	0.492	1.042	----	----	-----	-----
Bi	-----	-----	----	----	0.439	----	-----	-----	-----	-----
Σ	0.986	0.960	0.956	1.029	0.931	1.051	3.791	3.779	3.791	3.735
Σ *apfu*	4	4	4	4	4	4	11	11	11	11

* Drill core SP–32, 54.5–55.0 m. Other X-ray lines (standards in parentheses) than those described in Cabral *et al.* (2001) were used: As$L\alpha$ (InAs), Pb$L\beta$ (PbTe) and Bi$L\alpha$ (Bi). Micro-analyses: 1-4: Atheneite crystals attached to Au–Pd–Hg. 5: Pd–Se–Bi phase included in Au–Pd–Hg (Fig. 3e); its empirical formula approaches $Pd_3(Se,Bi)$. 6: Pd–Se–Hg phase attached to Au–Pd–Hg; its empirical formula is close to $(Pd,Hg)_3Se$. 7–10: Isomertieite crystals associated with Pd-poor gold. n.a.: not analyzed.

within the "Au_7Pd". It is remarkable that xenotime is sporadically included in the goethite coating (Fig. 3a). The goethite coating has patches enriched in palladium with no recognizable inclusions of native palladium, suggesting the existence of a Pd-bearing iron oxyhydroxide or hydroxide.

Elefante Prospect: Veinlet of Native Platinum and Associated *PGM*

The coarse-grained, arborescent aggregates of palladian gold described above were picked from deeply weathered, disaggregated and powdery material, and hence their relation to the host rock could not be determined. Evidence from relatively fresh material comes from the Elefante prospect, about 2 km south–southwest of Serra Pelada. A dark chlorite phyllite (drillcore EL–03, 31.5 m) is cross-cut by a veinlet of native platinum 20 μm wide, with which coarse-grained gold aggregates, as well as native palladium, Pd–Sb–As and Pd–Cu–O phases, and a Cu selenide are associated.

The host rock is a carbonaceous, white mica – quartz – chlorite phyllite, with traces of titanium oxide (rutile?) and zircon. Two generations of chlorite are recognized: an early, ferroan clinochlore [Fe/(Fe + Mg) ≈ 0.3] is

TABLE 8. ELECTRON-MICROPROBE DATA ON NATIVE PALLADIUM*, SERRA PELADA Au–Pd–Pt DEPOSIT, NORTHERN BRAZIL

	1	2	3	4	5	6	7
Pd wt.%	97.75	97.82	99.66	98.22	90.66	99.76	99.24
Au	1.46	2.22	0.77	1.01	1.49	1.35	0.62
Pt	<0.30	<0.30	<0.30	<0.30	0.31	<0.30	<0.30
Cu	0.15	<0.07	<0.07	<0.07	<0.07	<0.07	<0.07
Fe	0.06	0.51	0.34	0.40	0.19	0.50	0.49
As	<0.15	0.42	<0.15	<0.15	7.22	<0.15	0.40
Total	99.42	100.97	100.77	99.63	99.87	101.61	100.75
Pd at.%	98.92	97.25	98.94	98.69	88.66	98.34	98.18
Au	0.75	1.16	0.41	0.55	0.79	0.72	0.33
Pt	-----	-----	-----	0.00	0.17	-----	-----
Cu	0.22	-----	-----	-----	-----	-----	-----
Fe	0.11	0.95	0.64	0.77	0.35	0.94	0.92
As	-----	0.64	-----	-----	10.03	-----	0.56

* Drill core SP–32, 54.5–55.0 m. Micro-analyses 6 and 7 were done using As$L\alpha$ (InAs as standard).

TABLE 9. ELECTRON-MICROPROBE DATA ON PALLADIUM OXYGEN COMPOUNDS, SERRA PELADA Au–Pd–Pt DEPOSIT AND ELEFANTE PROSPECT

	1	2	3	4	5	6	7*	8*
Pd wt.%	65.74	67.65	67.64	78.09	80.15	80.00	47.11	48.52
Sc	4.06	3.83	4.15	<0.20	<0.20	<0.20	n.a.	n.a.
Au	<0.20	<0.20	<0.20	7.17	3.50	2.21	n.a.	n.a.
Pt	20.23	18.95	19.92	<0.20	<0.20	<0.20	n.a.	n.a.
Cu	<0.03	0.27	0.04	0.19	1.75	1.36	34.74	34.76
Hg	1.11	0.96	0.86	4.45	1.74	0.60	<0.20	<0.20
Fe	0.12	0.18	0.39	<0.03	0.08	0.17	0.30	0.38
Mn	0.95	0.89	0.97	1.10	2.59	3.66	0.02	0.03
Cl	0.05	<0.03	<0.03	0.08	0.16	0.46	0.06	0.10
O	5.84	4.95	4.14	7.31	9.11	11.29	16.29	14.58
Total	98.10	97.68	98.11	98.39	99.08	99.75	98.52	98.37
Pd at.%	53.09	56.84	58.89	57.61	52.66	47.72	21.99	23.69
Sc	4.38	4.38	4.91	-----	-----	-----	-----	-----
Au	-----	-----	-----	2.83	1.26	0.70	-----	-----
Pt	8.93	8.67	9.44	-----	-----	-----	-----	-----
Cu	-----	0.36	0.09	0.23	1.96	1.33	27.15	28.42
Hg	0.52	0.45	0.37	1.73	0.63	0.19	-----	-----
Fe	0.17	0.27	0.65	-----	0.07	0.19	0.25	0.35
Mn	1.46	1.43	1.67	1.57	3.29	4.25	0.02	0.03
Cl	0.09	-----	-----	0.16	0.35	0.82	0.10	0.15
O	31.36	27.61	23.98	35.87	39.79	44.80	50.52	47.36

* The mineral was analyzed for oxygen under 20 kV and 40 nA using the $K\alpha$ emission line and Al_2O_3 as the standard. Where not asterisked (micro-analyses 1–6), the concentration of oxygen was measured according to the analytical conditions described in Cabral *et al.* (2001). Micro-analyses 1–3: Alteration halo on Pd–Pt–Se phase. 4: Alteration halo on Pd arsenide. 5–6: Pd–O compound associated with native palladium. (Serra Pelada, drill core SP–32, 54.5–55.0 m). Micro-analyses 7–8: Pd–Cu–O phase in association with merlieite-II (Elefante Prospect, drill core EL–03, 31.5 m). n.a.: not analyzed.

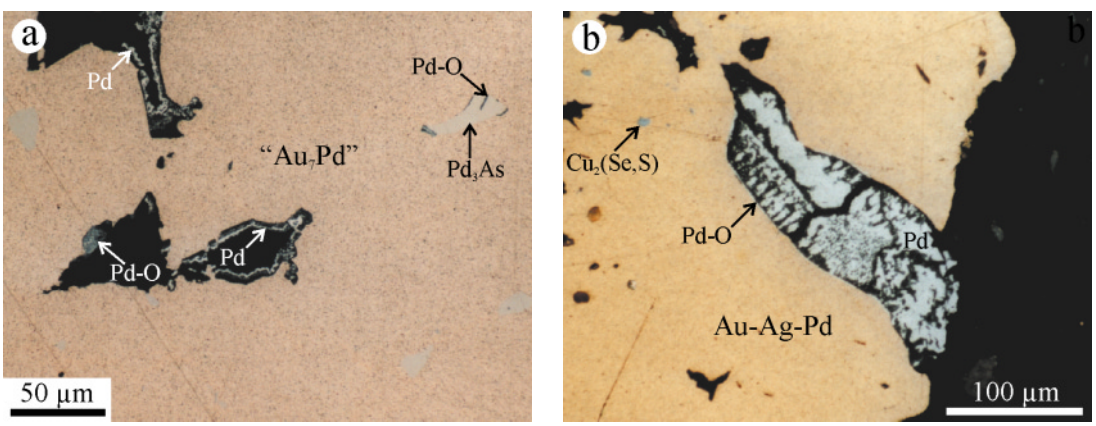

FIG. 4. Reflected-light photomicrographs illustrating the relationships of native palladium (Pd) and a Pd–O phase in palladian gold from Serra Pelada (a) and the Elefante prospect (b). a. Stripes of native palladium (white), associated with a Pd–O phase (dark grey), line vugs filled by goethite (black). Note incipient stage of Pd–O formation in a crystal of "guanglinite"(Pd_3As). b. Native palladium with parallel segments of a Pd–O phase. Black: gangue.

replaced by clinochlore [Fe/(Fe + Mg) ≈ 0.06]. A white-mica-rich alteration zone of about 1 cm in width envelops the veinlet of native platinum. The veinlet has a reddish halo of iron oxide.

The veinlet of native platinum consists of very fine-grained platinum crystals, less than 3 μm across, intermingled with a Mg-rich aluminosilicate (clinochlore?). Enveloped by a goethite–hematite halo, the veinlet cuts vein quartz with inclusions of Ti oxide and a $Cu_2(Se,S)$ phase of bluish tint, identified as berzelianite (Fig. 5a). An accurate electron-microprobe analysis of the native platinum could not be made owing to the small grain-size and poor quality of polish. The composition, recalculated to 100% and shown in Table 10, is noteworthy because of the low contents of iron and copper.

Gold occurs adjacent to the native platinum veinlet as anhedral crystals and aggregates up to 2 mm long. It is made up of 96.6 ± 1.1 wt.% Au, 2.2 ± 0.2% Ag, 0.8 ± 0.3% Cu, and 0.39 ± 0.02% Pd (Table 11). The gold contains inclusions of Ti oxide, subhedral to euhedral, 5 μm-long crystals of $Cu_2(Se,S)$, and palladium antimonides. The palladium antimonides have compositions close to mertieite-II and isomertieite (Table 12).

TABLE 10. ELECTRON-MICROPROBE DATA ON NATIVE PLATINUM, ELEFANTE PROSPECT*, NORTHERN BRAZIL

	1	2	3	4	5
Pt wt.%	71.22	87.37	84.12	87.15	91.99
Pd	15.58	3.52	6.76	5.75	1.57
Fe	1.21	0.90	1.09	1.47	n.a.
Cu	3.51	<0.07	0.08	<0.07	<0.07
Total	91.52	91.79	92.05	94.37	93.56
		Recalculated to 100%			
Pt	77.8	95.2	91.4	92.3	98.3
Pd	17.0	3.8	7.3	6.1	1.7
Fe	1.3	1.0	1.2	1.6	-----
Cu	3.8	-----	0.1	-----	0.0

* Drill core EL–03, 31.5 m. n.a.: not analyzed.

TABLE 11. ELECTRON-MICROPROBE DATA ON NATIVE PLATINUM, VEINLET-RELATED GOLD, ELEFANTE PROSPECT*, NORTHERN BRAZIL

	1	2	3	4	5	6	7	8
Au wt.%	95.58	95.85	97.97	95.28	97.51	97.98	95.94	96.75
Ag	2.33	2.32	1.88	2.52	2.12	1.99	2.25	2.35
Cu	1.04	0.94	0.42	0.97	0.61	0.41	0.92	0.91
Pd	0.40	0.41	0.41	0.39	0.38	0.37	0.38	0.41
Sb	<0.03	0.06	<0.03	<0.03	<0.03	<0.03	<0.03	<0.03
Total	99.35	99.58	100.68	99.16	100.62	100.75	99.49	100.42
Au at.%	92.08	92.29	94.69	91.96	93.78	94.60	92.60	92.48
Ag	4.10	4.08	3.32	4.44	3.72	3.51	3.97	4.10
Cu	3.11	2.81	1.26	2.90	1.82	1.23	2.75	2.70
Pd	0.71	0.73	0.73	0.70	0.68	0.66	0.68	0.73
Sb	-----	-----	0.09	-----	-----	-----	-----	-----

* Drill core EL–03, 31.5 m.

Native palladium is attached to, or partially enclosed in, gold, and has virtually no impurities, except for traces of copper (Table 12). The native palladium shows an intimate relationship with a low-reflectance phase resembling goethite in reflected light. This phase is a Pd–Cu–O compound that sporadically occurs in parallel arrays perpendicular to the margins of the host native palladium (Fig. 4b). A relic of mertieite-II is preserved at the margin of a Pd–Cu–O grain that encloses a Pd–Hg alloy (Fig. 5b, Table 12). The empirical formula is close to (Cu,Pd)O (Table 9, anal. 7 and 8).

Discussion

Dendrites of palladian gold

Because the Serra Pelada *garimpo* is located in a lateritic profile, supergene processes have been suggested to account for the bonanza near-surface mineralization (Meireles & Silva 1988, Tallarico *et al.* 2000, Moroni *et al.* 2001). However, the investigation of the coarse-grained dendrites of palladian gold has revealed *PGM* assemblages having an As–Sb–Se–Hg signature characteristic of epithermal deposits (Lindgren 1928). Significantly, most selenide minerals are deposited between 300° and 65°C (Simon *et al.* 1997). The Se signature of the Serra Pelada mineralization has been emphasized by Şener *et al.* (2002).

The weathering of gold particles under lateritic conditions leads to the development of an Au-rich, Ag-depleted halo (*e.g.*, Mann 1984, Colin & Vieillard 1991, Freyssinet *et al.* 1989, Minko *et al.* 1992, Colin *et al.* 1997), and ultimately, to the formation of grains of com-

TABLE 12. ELECTRON-MICROPROBE DATA ON PGM FROM THE ELEFANTE PROSPECT*, NORTHERN BRAZIL

	1	2	3	4	5	6	7	8
Pd wt.%	72.48	72.96	72.04	72.96	71.75	44.08	100.37	100.52
Au	0.59	0.33	<0.30	<0.30	2.64§	<0.30	<0.30	<0.30
Ag	<0.20	<0.20	<0.20	<0.20	<0.20	0.88	<0.20	<0.20
Hg	<0.20	<0.20	<0.20	<0.20	<0.20	50.46	<0.20	<0.20
Sb	24.82	24.69	24.72	24.83	16.08	<0.03	<0.03	<0.03
As	3.09	3.30	3.22	3.22	8.66	<0.10	<0.10	<0.10
Cu	0.48	0.16	0.75	0.34	3.75	4.63	0.18	0.22
Sn	0.08	0.10	0.07	0.09	0.06	<0.03	<0.03	<0.03
Total	101.54	101.54	100.80	101.44	102.94	100.05	100.55	100.74
Pd	7.992	8.045	7.961	8.035	10.166	1.663	0.997	0.996
Au	0.035	0.020	-----	-----	0.202	-----	-----	-----
Cu	0.089	0.030	0.139	0.063	0.890	0.293	0.003	0.004
Ag	-----	-----	-----	-----	-----	0.032	-----	-----
ΣPd	8.116	8.095	8.100	8.098	11.258	1.988	1.000	1.000
Sb	2.392	2.379	2.388	2.390	1.991	-----	-----	-----
As	0.484	0.517	0.505	0.504	1.743	-----	-----	-----
Sn	0.008	0.010	0.007	0.009	0.008	-----	-----	-----
ΣSb	2.884	2.906	2.900	2.903	3.742	-----	-----	-----
Hg	-----	-----	-----	-----	-----	1.012	-----	-----
Σ *apfu*	11	11	11	11	15	3	1	1

* Drill core EL–03, 31.5 m. § Probably due to contamination from the surrounding gold matrix. Micro-analyses 1–4: mertieite-II, 5: isomertieite, 6: Pd–Hg alloy found as inclusion (relic?) in the Pd–Cu–O phase of Figure 5b, 7–8: native palladium associated with Pd–Cu–O phase

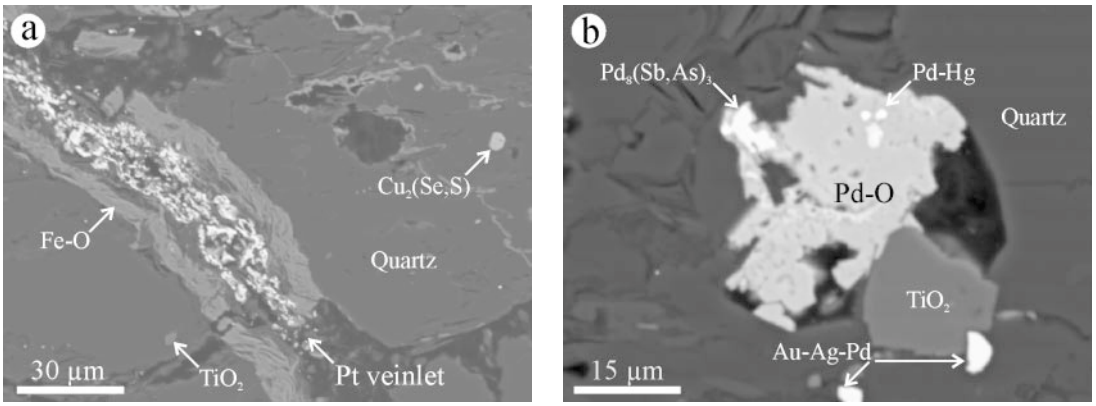

FIG. 5. BSE images, Elefante prospect. a. Veinlet of native platinum cuts vein quartz containing inclusions of TiO_2 and berzelianite crystals, $Cu_2(Se,S)$. The veinlet has a halo of goethite–hematite (Fe–O). See Table 10 for results of micro-analyses. b. Pd–O phase with relics of mertieite-II and inclusions of a Pd–Hg alloy. For results of micro-analyses, see Table 9 (anal. 7 and 8) and Table 12 (anal. 1 and 6).

positionally pure, supergene gold (*e.g.*, Boyle 1979, Mann 1984, Oliveira & Campos 1991, Santosh & Omana 1991, Lawrance & Griffin 1994). Like silver, palladium also is leached from gold alloy during weathering (Varajão *et al.* 2000). In fact, some crystals of "Au_7Pd" have a thin, discontinuous, Pd-depleted rim, and pure gold occurs as tiny crystals and marginal veinlets, but is very minor. Therefore, the dendritic aggregates of palladian gold appear to be only weakly affected by weathering, and are more likely residual components of a primary, hydrothermal mineralization. In this connection, it is worth mentioning that dendritic gold is known to occur in epithermal and hot-spring gold deposits (Saunders 1994, Sherlock & Lehrman 1995). Also, the dendritic aggregates of Pt–Pd and Pd–Hg–Au alloys from the Bom Sucesso stream, Minas Gerais, possibly result from open-space infill by low-temperature hydrothermal fluids (Cassedanne *et al.* 1996, Fleet *et al.* 2002).

Se-bearing phases

Sparse crystals of palladseite and sudovikovite are included in palladian gold. These very rare selenide minerals occur in the hematite-rich auriferous veins (*jacutinga*) at the Cauê iron-ore mine, Minas Gerais, Brazil (Davis *et al.* 1977, Olivo & Gauthier 1995, Kwitko *et al.* 2002, Cabral *et al.* 2002b). Like at Serra Pelada, the jacutinga-style mineralization is characterized by (i) palladian gold (Hussak 1904) and (ii) a metal assemblage typical of epithermal deposits (Cabral *et al.* 2002b).

The Pd–Se phase seems to be a new *PGM*, as there are no reports in the literature of a natural compound analogous to the synthetic Pd_9Se_2. This unidentified species is an alloy, rather than a selenide, as its Se content is too low to account for charge balance in relation to Pd. It is interesting to note that a Pd–Cu–Se alloy consisting of 85 at.% Pd, 8% Cu and 7% Se was found at Ruwe and Shinkolobwe, Congo, where palladian gold, native palladium and $PtSe_2$ (sudovikovite?) also occur (Jedwab 1997). The possibility that the Pd–Se phase corresponds to synthetic Pd_9Se_2 raises the question whether the phase-equilibrium relationships in the system Pd–Se can be applied to natural systems. Pd_9Se_2 apparently is stable between 635 and 390°C (Okamoto 1992), but such a temperature range is far above the suggested temperature of formation (<300°C) of the Serra Pelada mineralization (Şener *et al.* 2002).

A Pd–Hg–Se phase was observed at the margins of the Au–Pd–Hg alloy. Note that micro-analytical data suggest the empirical formula $(Pd,Hg,Pb)_3Se$, raising the question whether there is a compositional series between Se- and As-rich (atheneite) end-members. More importantly, however, a Pd–Hg–Se association is known from Au–Se-bearing hydrothermal veins (Mernagh *et al.* 1994, Paar *et al.* 1998, Nickel 2002, Stanley *et al.* 2002), for which a temperature of formation of about 100°C has been proposed (Simon *et al.* 1997).

Native palladium

The native palladium from both Serra Pelada and the Elefante prospect is virtually pure. Nekrasov (1996, p. 85) pointed out that auriferous native palladium, even with only 1 to 2 wt.% Au, is extremely rare. It seems to have exclusively been recorded from Itabira, Minas Gerais, Brazil, with 2 wt % Au (Olivo & Gauthier 1995). In the Kupferschiefer deposits of Poland, nearly pure

native palladium forms intergrowths (<10 μm) with Pd–Pt-bearing argentiferous gold (Kucha 1981).

The native palladium masses of both the Serra Pelada and Elefante areas are intimately associated with a Pd–O-bearing phase. Microstructural evidence indicates that part of such a Pd–O compound formed at the expense of a precursor Pd mineral (*e.g.*, Pd–Se alloy, mertieite-II; Figs. 3d, 5b). The Pd–O-bearing phase was possibly susceptible to variable pH and Eh conditions due to oscillations of the water table. Where conditions were compatible with the stability field of palladium, native palladium would have formed from the Pd–O phase (*cf.* stability diagrams of Bowles 1986, Wood *et al.* 1989, Olivo & Gammons 1996). On the other hand, the presence of some mercury in the Pd–O-bearing phase may also suggest involvement of a low-temperature hydrothermal fluid. Some spongy masses of native palladium are similar to those of native platinum and Pt–Pd alloy documented from the Waterberg deposit, South Africa (Wagner 1929, McDonald *et al.* 1999). In this case, crystallization of native palladium from an amorphous Pd–O precursor could have occurred under temperatures within the epithermal range (McDonald *et al.* 1999). The parallel array of a Pd–O phase in native palladium (Fig. 4b) could be interpreted as relics of desiccation cracks from which native palladium crystallized (*i.e.*, oxygen loss and dehydration leading to cracking of amorphous Pd–O).

Veinlet of native platinum

Whereas it contains significant amounts of palladium, the native platinum is poor in iron and copper, and resembles the virtually Fe–Cu-free Pt–Pd alloy from the hematite veins and hematite replacement zones of the Waterberg deposit (Wagner 1929, McDonald *et al.* 1999). A rim of native platinum around a Pt–Fe alloy from the Baimka placer deposit, Russian Far East, is also nearly devoid of Cu and Fe (Gornostayev *et al.* 1999). These observations on natural alloys confirm the experimental evidence that under low fugacity of sulfur and low-temperature conditions, grains of platinum alloy are poor in Fe (Evstigneeva & Tarkian 1996).

Concluding Remarks

The coarse-grained aggregates of palladian gold from Serra Pelada display four compositional types of gold, with distinct mineral assemblages: i) "Au_7Pd", the most abundant Au–Pd alloy, hosts Pd arsenides ("guanglinite" and Sb-bearing "guanglinite"), Pd–Pt–Se and Pd–Se phases, sudovikovite and palladseite, ii) Au–Pd–Hg alloy, characteristically with atheneite and rarely observed Pb-bearing Pd–Hg–Se and Pd–Bi–Se phases, iii) Pd-poor gold – isomertieite – Mn–Ba oxide assemblage, and iv) pure gold–goethite assemblage.

The paragenetic relationships among the gold–*PGM* assemblages cannot be established, but the Pd-poor gold assemblage is possibly later than the Au–Pd–Hg alloy. Whatever the case, subsequent removal of As, Sb and Se from *PGM* led to the formation of Pd–O-bearing compounds, either by low-temperature hydrothermal or supergene fluids. Oxygen loss and dehydration of Pd–O masses would account for the spongy masses of native palladium, occasionally with cracks and parallel arrays of Pd–O.

Acknowledgements

ARC has benefitted from a DAAD (*Deutscher Akademischer Austauschdienst*) scholarship. This contribution would have not been possible without the cooperation of *Companhia Vale do Rio Doce* (CVRD), particularly of Paulo R. Amorim dos Santos Lima (*Paulão*), in providing access to the *garimpo* area and to the drill cores, polished sections and private reports. Thanks are also due to Klaus Herrmann (TU Clausthal) for his meticulous assistance with the electron-microprobe analyses. Chris Stanley and an anonymous reviewer are gratefully acknowledged for the constructive comments. The careful editorial handling by Robert F. Martin is also deeply appreciated.

References

Bowles, J.F.W. (1986): The development of platinum-group minerals in laterites. *Econ. Geol.* **81**, 1278-1285.

Boyle, R.W. (1979): The geochemistry of gold and its deposits. *Geol. Survey Can., Bull.* **280**.

Cabral, A.R., Lehmann, B., Kwitko, R. & Cravo Costa, C.H. (2002a): The Serra Pelada Au–Pd–Pt deposit, Carajás mineral province, northern Brazil: reconnaissance mineralogy and chemistry of very-high-grade palladian gold mineralization. *Econ. Geol.* **97**, 1127-1138.

_____, _____, _____, Galbiatti, H.F. & Pereira, M.C. (2002b): Palladseite and its oxidation: evidence from Au–Pd vein-type mineralization (jacutinga), Cauê iron-ore mine, Quadrilátero Ferrífero, Minas Gerais, Brazil. *Mineral. Mag.* **66**, 327-336.

_____, _____, _____, Jones, R.D., Pires, F.R.M., Rocha Filho, O.G. & Innocentini, M.D. (2001): Palladium–oxygenated compounds of the Gongo Soco mine, Quadrilátero Ferrífero, central Minas Gerais, Brazil. *Mineral. Mag.* **65**, 169-179.

Cabri, L.J. & Laflamme, J.H.G. (1981): Analyses of minerals containing platinum-group elements. *In* Platinum-Group Elements: Mineralogy, Geology, Recovery (L.J. Cabri, ed). *Can. Inst. Mining Metall., Spec. Vol.* **23**, 151-173.

Cassedanne, J.P., Jedwab, J. & Alves, J.N. (1996): Apport d'une prospection systématique à l'étude de l'origine de l'or et du platine alluviaux du Córrego Bom Sucesso (Serro – Minas Gerais). *An. Acad. Bras. Ciências* **68**, 569-82.

COLIN, F., SANFO, Z., BROWN, E., BOURLÈS, D. & MINKO, A.E. (1997): Gold: a tracer of the dynamics of tropical laterites. *Geology* **25**, 81-84.

_____ & VIEILLARD, P. (1991): Behavior of gold in the lateritic equatorial environment: weathering and surface dispersion of residual gold particles, at Dondo Mobi, Gabon. *Appl. Geochem.* **6**, 279-290.

CUNHA, B.C.C., SANTOS, D.B. & PRADO, P. (1984): Contribuição ao estudo da estratigrafia da região de Gradaús, com ênfase no Grupo Rio Fresco. *In* Anais do 33. Congresso Brasileiro de Geologia (Rio de Janeiro) **2**, 873-885.

DARDENNE, M.A. & SCHOBBENHAUS, C. (2001): *Metalogênese do Brasil*. Editora Universidade de Brasília, Brasília, Brazil.

DAVIS, R.J., CLARK, A.M. & CRIDDLE, A.J. (1977): Palladseite, a new mineral from Itabira, Minas Gerais, Brazil. *Mineral. Mag.* **41**, 123, M10-M13.

DIELLA,V., FERRARIO, A. & GIRARDI, V.A.V. (1995): PGE and PGM in the Luanga mafic-ultramafic intrusion in Serra dos Carajás (Pará State, Brazil). *Ore Geol. Rev.* **9**, 445-453.

DOCEGEO, EQUIPE-DISTRITO AMAZÔNIA (1988): Revisão litoestratigráfica da Província Mineral de Carajás. In: Província Mineral de Carajás – Litoestratigrafia e principais depósitos minerais. *In* Anexo do 35. Congresso Brasileiro de Geologia (Belém), 11-56.

EVSTIGNEEVA, T. & TARKIAN, M. (1996): Synthesis of platinum-group minerals under hydrothermal conditions. *Eur. J. Mineral*. **8**, 549-564.

FLEET, M.E., DE ALMEIDA, C.M. & ANGELI, N. (2002): Botryoidal platinum, palladium and potarite from the Bom Sucesso stream, Minas Gerais, Brazil: compositional zoning and origin. *Can. Mineral.* **40**, 341-355.

FREYSSINET, P., ZEEGERS, H. & TARDY, Y. (1989): Morphology and geochemistry of gold grains in lateritic profiles of southern Mali. *J. Geochem. Expl.* **32**, 17-31.

GORNOSTAYEV, S.S., CROCKET, J.H., MOCHALOV, A.G. & LAAJOKI, K.V.O. (1999): The platinum-group minerals of the Baimka placer deposits, Aluchin Horst, Russian Far East. *Can. Mineral.* **37**, 1117-1129.

HUSSAK, E. (1904): Über das Vorkommen von Palladium und Platin in Brasilien. *Sitzungsberichte der mathematisch-naturwissenschaftlichen Klasse der Kaiserlichen Akademie der Wissenschaften* **113**, 379-468.

JEDWAB, J. (1997): Minéralogie des métaux du groupe du platine au Shaba, Zaïre. *In* Colloque International Cornet, Académie Royale des Sciences d'Outre-Mer, 325-355.

KUCHA, H. (1981): Precious metal alloys and organic matter in the Zechstein copper deposits, Poland. *Tschermaks Mineral. Petrogr. Mitt.* **28**, 1-16.

KWITKO, R., CABRAL, A.R., LEHMANN, B., LAFLAMME, J.H.G., CABRI, L.J., CRIDDLE, A.J. & GALBIATTI, H.F. (2002): Hongshiite, PtCu, from itabirite-hosted Au–Pd–Pt mineralization (jacutinga), Itabira district, Minas Gerais, Brazil. *Can. Mineral.* **40**, 711-723.

LAWRANCE, L.M. & GRIFFIN, B.J. (1994): Crystal features of supergene gold at Hannan South, Western Australia. *Mineral. Deposita* **29**, 391-398.

LINDGREN, W. (1928): *Mineral Deposits* (3rd ed.). McGraw Hill, New York, N.Y.

MACHADO, N., LINDENMAYER, Z., KROGH, T.E. & LINDENMAYER, D. (1991): U–Pb geochronology of Archean magmatism and basement reactivation in the Carajás area, Amazon shield, Brazil. *Precamb. Res.* **49**, 329-354.

MANN, A.W. (1984): Mobility of gold and silver in lateritic weathering profiles: some observations from Western Australia. *Econ. Geol.* **79**, 38-49.

MCDONALD, I., OHNENSTETTER, D., ROWE, J.P., TREDOUX, M., PATTRICK, R.A.D. & VAUGHAN, D.J. (1999): Platinum precipitation in the Waterberg deposit, Naboomspruit, South Africa. *S. Afr. J. Geol.* **102**, 184-191.

MEIRELES, E.M. & SILVA, A.R.B. (1988): Depósito de ouro de Serra Pelada, Marabá, Pará. *In* Principais Depósitos Minerais do Brasil **3** (C. Schobbenhaus C & C.E.S. Coelho, eds.). Departamento Nacional da Produção Mineral, Companhia Vale do Rio Doce, Brasília, Brazil (547-557).

MERNAGH, T.P., HEINRICH, C.A., LECKIE, J.F., CARVILLE, D.P., GILBERT, D.J., VALENTA, R.K. & WYBORN, L.A.I. (1994): Chemistry of low-temperature hydrothermal gold, platinum, and palladium (±uranium) mineralization at Coronation Hill, Northern Territory, Australia. *Econ. Geol.* **89**, 1053-1073.

MINKO, A.E., COLIN, F., TRESCASES, J.-J. & LECOMTE, P. (1992): Altération latéritique du gîte aurifère d'Ovala (Gabon), et formation d'une anomalie superficielle de dispersion. *Mineral. Deposita* **27**, 90-100.

MORONI, M., GIRARDI, V.A.V. & FERRARIO, A. (2001) The Serra Pelada Au–PGE deposit, Serra dos Carajás (Pará State, Brazil): geological and geochemical indications for a composite mineralising process. *Mineral. Deposita* **36**, 768-785.

NEKRASOV, I.YA. (1996): *Geochemistry, Mineralogy and Genesis of Gold Deposits*. Balkema, Rotterdam, The Netherlands.

NICKEL, E.H. (2002): An unusual occurrence of Pd, Pt, Au, Ag, and Hg minerals in the Pilbara region of Western Australia. *Can. Mineral.* **40**, 419-433.

OKAMOTO, H. (1992): The Pd–Se (palladium–selenium) system. *J. Phase Equilibria* **13**, 69-72.

OLIVEIRA, S.M.B. & CAMPOS, E.G. (1991): Gold-bearing iron duricrust in Central Brazil. *J. Geochem. Explor.* **41**, 309-323.

OLIVO, G.R. & GAMMONS, C.H. (1996): Thermodynamic and textural evidence for at least two stages of Au–Pd mineralization at the Cauê iron mine, Itabira district, Brazil. *Can. Mineral.* **34**, 547-557.

_____ & GAUTHIER, M. (1995): Palladium minerals from the Cauê iron mine, Itabira district, Minas Gerais, Brazil. *Mineral. Mag.* **59**, 455-463.

PAAR, W.H., ROBERTS, A.C., CRIDDLE, A.J. & TOPA, D. (1998): A new mineral, chrisstanleyite, $Ag_2Pd_3Se_4$, from Hope's Nose, Torquay, Devon, England. *Mineral. Mag.* **62**, 257-264.

PINHEIRO, R.V.L. & HOLDSWORTH, R.E. (1997a): Reactivation of Archaean strike-slip fault systems, Amazon region, Brazil. *J. Geol. Soc. London* **154**, 99-103.

_____ & _____ (1997b): The structure of the Carajás N–4 Ironstone deposit and associated rocks: relationship to Archaean strike-slip tectonics and basement reactivation in the Amazon region, Brazil. *J. S. Am. Earth Sci.* **10**, 305-319.

SANTOSH, M. & OMANA, P.K. (1991): Very high purity gold from lateritic weathering profiles of Nilambur, southern India. *Geology* **19**, 746-749.

SAUNDERS, J.A. (1994): Silica and gold textures in bonanza ores of the Sleeper deposit, Humboldt County, Nevada: evidence for colloids and implications for epithermal ore-forming processes. *Econ. Geol.* **89**, 628-638.

ŞENER, A.K., GRAINGER, C.J. & GROVES, D.I. (2002): Epigenetic gold–platinum-group element deposits: examples from Brazil and Australia. *Trans. Inst. Mining Metall.* **111**, B65-B73.

SHERLOCK, R.L. & LEHRMAN, N.J. (1995): Occurrences of dendritic gold at the McLaughlin mine hot-spring deposit. *Mineral. Deposita* **30**, 323-327.

SIMON, G., KESLER, S.E. & ESSENE, E.J. (1997): Phase relations among selenides, sulfides, tellurides, and oxides. II. Applications to selenide-bearing ore deposits. *Econ. Geol.* **92**, 468-484.

STANLEY, C.J., CRIDDLE, A.J., FÖRSTER, H.-J. & ROBERTS, A.C. (2002): Tischendorfite, $Pd_8Hg_3Se_9$, a new mineral species from Tilkerode, Harz Mountains, Germany. *Can. Mineral.* **40**, 739-745.

SUITA, M.T.F. & NILSON, A.A. (1988): Geologia do complexo máfico-ultramáfico Luanga (Província de Carajás, Pará) e das unidades encaixantes. *In* Anais do 35. Congresso Brasileiro de Geologia (Belém), 2813-2823.

TALLARICO, F.H.B., COIMBRA, C.R. & CRAVO COSTA, C.H. (2000): The Serra Leste sediment-hosted Au–(Pd–Pt) mineralization, Carajás Province. *Revista Brasileira de Geociências* **30**, 226-229.

VARAJÃO, C.A.C., COLIN, F., VIEILLARD, P., MELFI, A.J. & NAHON, D. (2000): Early weathering of palladium gold under lateritic conditions, Maquiné mine, Minas Gerais, Brazil. *Appl. Geochem.* **15**, 245-263.

VASCONCELOS, P.M., RENNE, P.R., BRIMHALL, G.H. & BECKER, T.A. (1994): Direct dating of weathering phenomena by $^{40}Ar/^{39}Ar$ and K–Ar analysis of supergene K–Mn oxides. *Geochim. Cosmochim. Acta* **58**, 1635-1665.

VILLAS, R.N. & SANTOS, M.D. (2001): Gold deposits of the Carajás mineral province: deposit types and metallogenesis. *Mineral. Deposita* **36**, 300-331.

WAGNER, P.A. (1929): *The Platinum Deposits and Mines of South Africa*. Oliver and Boyd, Edinburgh, U.K.

WOOD, S.A., MOUNTAIN, B.W. & FENLON, B.J. (1989): Thermodynamic constraints on the solubility of platinum and palladium in hydrothermal solutions: reassessment of hydroxide, bisulfide, and ammonia complexing. *Econ. Geol.* **84**, 2020-2028.

Received May 5, 2002, revised manuscript accepted September 10, 2002.